Optimal Placement and Sizing of Active Power Filters in RDS Using TLBO for Harmonic Distortion Reduction

Ashokkumar Lakum, Deepak Bhonsle, and Mahesh Pandya

Abstract This paper focuses the optimal placement and sizing (OPAS) of active power filters (APFs) in a radial distribution system (RDS) for harmonic reduction. The optimization problem is constrained and nonlinear. The placement of APFs is achieved through a recently developed technique called nonlinear load (NL) position-based current injection (NLPCI). The optimal size of APFs to reduce the total harmonic distortion in voltage (THD_V) to meet IEEE standards, a teaching-learning-based optimization (TLBO) algorithm is used, and its performance is compared to that of flower pollination (FPA) and bird swarm (BSA) algorithms. The results indicate that the TLBO outperforms the other algorithms in computational performance, as demonstrated using an IEEE 69-bus RDS with NL and nonlinear distributed generation (NLDG).

Keywords Active power filter · Power quality · Radial distribution system · Teaching-learning-based optimization

1 Introduction

Distributed generation (DG) is a key element of the smart grid. It has garnered significant attention due to its numerous benefits. One of the essential tasks is integrating DG into the radial distribution system (RDS). Power quality issues come from improper DG integration due to the harmonics generated by the converter [1]. A converter-based DG is referred to as a nonlinear DG (NLDG) when it introduces harmonics into the RDS [2]. Total harmonic distortion in voltage (THD_V) and individual harmonic distortion in voltage (IHD_V) should be less than 5% and 3%, respectively, by IEEE standard 519 [3]. Harmonics need to be controlled to meet this

A. Lakum (✉) · M. Pandya
Lukhdhirji Engineering College, Morbi, Gujarat, India
e-mail: aclakum@lecollege.ac.in

D. Bhonsle
C. K. Pithawla College of Engineering and Technology, Surat, Gujarat, India

A. Kumar et al. (eds.), *Decarbonisation and Digitization of the Energy System*, Lecture Notes in Electrical Engineering 1099, https://doi.org/10.1007/978-981-99-7630-0_22

criterion. The straightforward solution to mitigate harmonic distortion in RDS is to install active power filters (APFs) at all NL buses with current ratings equal to those of the respective NLs. But the price is rather exorbitant. As a result, an optimization approach is needed for APF location, rating, and cost [4].

Numerous algorithms, including genetic algorithm, variants of particle swarm optimization [5], harmony search [4], firefly algorithm, and grey wolf optimizer [6] algorithms have been utilized for optimal placement and sizing (OPAS) of APF. Most of the used algorithms have algorithmic-specific parameters. It is too difficult to tune these parameters for the different problems. Improper tuning of these parameters may give false results.

The theory of "No Free Lunch" states that no single optimization algorithm can be considered the best for all issues and that several algorithms can tackle a particular optimization problem [7]. For the same issue, a different optimization procedure produces a different outcome.

Considering this aspect, Prof. Rao et al. have developed the teaching–learning-based optimization (TLBO) algorithm, and it operates without algorithm-specific parameters [8]. It is used for OPAS of APF and compared with nature-inspired flower pollination algorithm (FPA) [9] and bio-inspired bird swarm algorithm (BSA) [10].

Below are the main contributions of this paper in relation to the OPAS of APF, taking into account the integration of NLDG and nonlinear load:

- The TLBO is coupled with harmonic load flow and used to find optimal size of APF.
- The three algorithms (TLBO, FPA, and BSA) that have different bases are compared and analyzed for two cases: NL and NL plus NLDG.
- To determine the size of APF in the presence of NL and NLDGs, the TLBO, FPA, and BSA algorithms were utilized. The computational tests were conducted in terms of the best value. The results indicated that the APF requirement is higher when the NLDG is integrated into the RDS as compared to without NLDG.
- The computational tests revealed that TLBO outperformed FPA and BSA by producing the minimum value of APF current in both cases.

In the next section TLBO is explained.

2 TLBO

A teacher's influence on students' performance in a class is the basis for the algorithm known as TLBO. It is based on the ideas of the teaching-learning process. The two essential elements of the algorithm are the teacher and the students, who characterize two fundamental modes of learning: learning from the teacher (known as the teacher phase) and engaging with other students (known as the learner phase). It is well explained in [8].

2.1 Teacher Phase

In this stage of the algorithm, the focus is on replicating the learning process of students with the aid of a teacher. The teacher imparts knowledge to the learners and strives to improve the overall performance of the class. If there are "*m*" subjects (or design variables) available to a population of "*n*" learners (with $k = 1, 2, \ldots$, n), then at each sequential teaching-learning cycle *i, Mj*, *i* represents the average performance of the learners in a particular subject "*j*" (where $j = 1, 2, \ldots, m$).

The algorithm selects the most knowledgeable and experienced individual in the population as the teacher, based on their performance across all subjects. This is denoted by $X_{total}k_{best,i}$, which represents the best learner's result across all subjects, and who will serve as the teacher for the current cycle. The teacher is expected to make maximum efforts to improve the knowledge level of the entire class. However, the quality of learning gained by each individual learner is influenced by the quality of teaching provided by the teacher and the learners' abilities. To account for this, the difference between the teacher's result and the mean result of the learners in each subject is calculated as follows:

$$Difference\_Mean_{j,i} = r_i(X_{j,kbest,i} - T_f M_{j,i}) \quad (1)$$

The difference between the teacher's result (X_j, $k_{best,i}$) in a given subject "*j*" and the mean result of the learners in that subject is expressed in the equation. The value of the teaching factor, T_f, determines the extent of change to the mean result, and is determined by a random number, $r_{i,}$ within the range of 0 to 1. T_f can take on a value of either 1 or 2, and its specific value is determined randomly.

$$T_f = round[1 + rand(0, 1)(2 - 1)] \quad (2)$$

The teaching factor (T_f) is not a fixed parameter in the TLBO algorithm and is not provided as an input. Instead, its value is randomly determined by the algorithm using Eq. (2).

$$X'_{j,k,i} = X_{j,k,i} + Difference\_Mean_{j,i} \quad (3)$$

During the teacher phase, based on $Difference\_Mean_{j,i}$ the existing solution is updated according to Eq. (3), where $X'_{j,k,i}$ represents the updated value of $X_{j,k,i}$. This updated value is accepted only if it leads to a better function value. All accepted function values at the end of the teacher phase are retained and used as input for the learner phase.

2.2 Learner Phase

In this stage of the algorithm, the focus is on simulating the learning process of students through interactions with one another. Learners have the opportunity to gain new knowledge by engaging in discussions and interactions with other learners. If one learner possesses more knowledge than another, the latter can learn from the former.

The next section deals with problem formulation. The simulated results are discussed later on and it is followed by the conclusion in the last.

3 Problem Formulation

RDS with NLs, NLDGs, and APFs are mathematically modeled as per [6]. The bus injection to branch current (BIBC) and branch current to the bus voltage (BCBV) based harmonic load flow is employed in the simulation [11]. Then it is coupled with the TLBO, FPA, and BSA.

3.1 Modeling of RDS

The RDS is modeled in terms of impedance, which includes the resistance and inductance of the RDS. It is calculated considering harmonics environment.

3.2 Modeling of Nonlinear Load

The representation of nonlinear load can be formulated by keeping the source of harmonic current injection as the base as shown in [5, 12]. The magnitude of rms nonlinear current is given below,

$$I_{nl}^{(h)} = I_{nl,r}^{(h)} + jI_{nl,im}^{(h)} \tag{4}$$

$$I_{\mathrm{nl}} = \sqrt{\sum_{h=2}^{H} (I_{nl,r}^{2(h)} + I_{nl,im}^{2(h)})} \tag{5}$$

Here, $I_{nl,r}^{(h)}$ is the real part of nonlinear current while $I_{nl,im}^{(h)}$ is the imaginary part of nonlinear current, I_{nl} indicates the rms value, the highest order of harmonics is H.

3.3 Modeling of APF

The APF is represented as a current source [5, 12]. Calculation of I_{apf} is done on the basis of net nonlinear current at PCC. Net nonlinear current (I_{nl}) is a vector addition of nonlinear currents of loads.

$$I_{apf} = k(I_{nl}) \tag{6}$$

Here, k is proportionate of net nonlinear current. It has the value such that *Iapf* satisfies the constraints.

APF is represented as a set of current sources. It injects different orders of harmonics at a PCC as per the value of k. The current of APF is expressed as

$$I_{apf}^{(h)} = I_{apf,r}^{(h)} + jI_{apf,im}^{(h)} \tag{7}$$

$$I_{apf} = \left[\sum_{h=2}^{H} (I_{apf,r}^{2(h)} + I_{apf,im}^{2(h)})\right]^{1/2} \tag{8}$$

Here, $I_{apf,r}^{(h)}$, $I_{apf,im}^{(h)}$, and I_{apf} are the real part, imaginary part, and the rms value of current of APF respectively.

3.4 Modeling of NLDG

The DG which is a current source [13, 14], supplies the nonlinear current into the system. The fundamental current is estimated [13] by power rating of the DG and therefore, NLDG harmonic current is calculated from spectrum as

$$I_{hdg}^{(h)} = K_{dg} I_{dg} \tag{9}$$

Here, $I_{hdg}^{(h)}$, K_{dg}, and I_{dg} are the harmonic current of DG, part of harmonic current as per the spectrum of DG, and the fundamental current of DG respectively.

3.5 Harmonic Load Flow

The bus injection to branch current (BIBC) and branch current to the bus voltage (BCBV) based harmonic load flow is used in this paper [11]. Then it is coupled with the optimization algorithm. THDv is calculated at all buses using harmonic load flow and it is essential for identification of critical buses which violates the standard limits.

The THD_V is given as,

$$THDv = \frac{\sqrt{\sum_{h=2}^{H} (IHDv)^2}}{V_f^1} \tag{10}$$

Here V_f^1 is fundamental frequency voltage.

From the value of THDv at all buses, the vital buses where the IEEE standard limits are not satisfied are found. It helps in deciding the policy to alleviate the harmonics; i.e. the placement and sizing of APF.

4 Optimization Process

The optimization algorithms are employed to determine the optimal size. The objective function is based on the APF current. Here the main objective is to reduce the APF current such that the constraints are satisfied. It is depicted as:

$$OF_{IFT} = \min \sum_{m=1}^{M} \sqrt{\sum_{h=2}^{H} \left| I_{apf,m}^{h} \right|^2} + DP \tag{11}$$

where, "*m*" represents the bus number, "*M*" represents the total number of buses, "*h*" denotes the order of harmonics, "*H*" represents the highest order of harmonics, and "*DP*" stands for a dynamic penalty.

Subjected to

$$THD_V - 0.05 \leq 0, THD_{Vindi} - 0.03 \leq 0, I_{apf} \leq I_{apf,MAX} \tag{12}$$

By using a black box approach, as illustrated in Fig. 1, TLBO has the advantage of analyzing a system. It offers the system with input variables, such as the current of APFs, and observes the resulting output, which is the objective function's value. The TLBO continues to adjust the inputs of the system based on the feedback it receives (output) until the specified end criteria are met. Figure 2 shows the flowchart for optimization process.

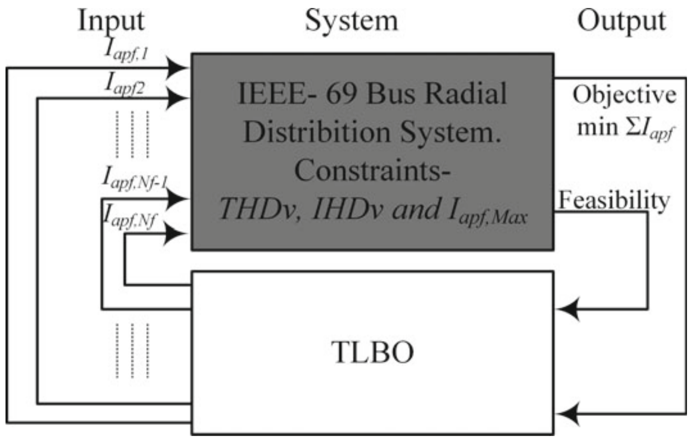

Fig. 1 Block diagram of TLBO for OPAS of APFs in RDS

5 Results Analysis

This section covers the result analysis.

5.1 *Initial Data*

The IEEE-69 bus [15] RDS with modifications is taken into account, for simulation (Fig. 3). Here, it is assumed that the NLDGs are connected to the NL buses. The NLs have a harmonic spectrum up to 49^{th} order of harmonics as per the six-pulse converter [16]. The NLDG exhibits a harmonic spectrum, as illustrated in Fig. 4 [17]. The NLs are placed at buses 27, 46, and 65, i.e., at end nodes.

To find the location of APF, here recently developed NL position-based APF current injection (NLPCI) technique is used [6].

Table 1 represents the situation of buses regarding the availability of APF. Here, all the possible combinations of APF allocation are considered. The NLs are at three buses. So, the possible combinations of APF allocation are (2^3–1 = 7) seven, viz. 1 through 7. The investigations are carried out for seven states as furnished in Table 1, wherein "+" denotes the availability of APF and "*" denotes its non-availability. For finding the rating of APF, the three algorithms viz. TLBO, FPA, and BSA are implemented to determine APF current in a manner that meets the constraints.

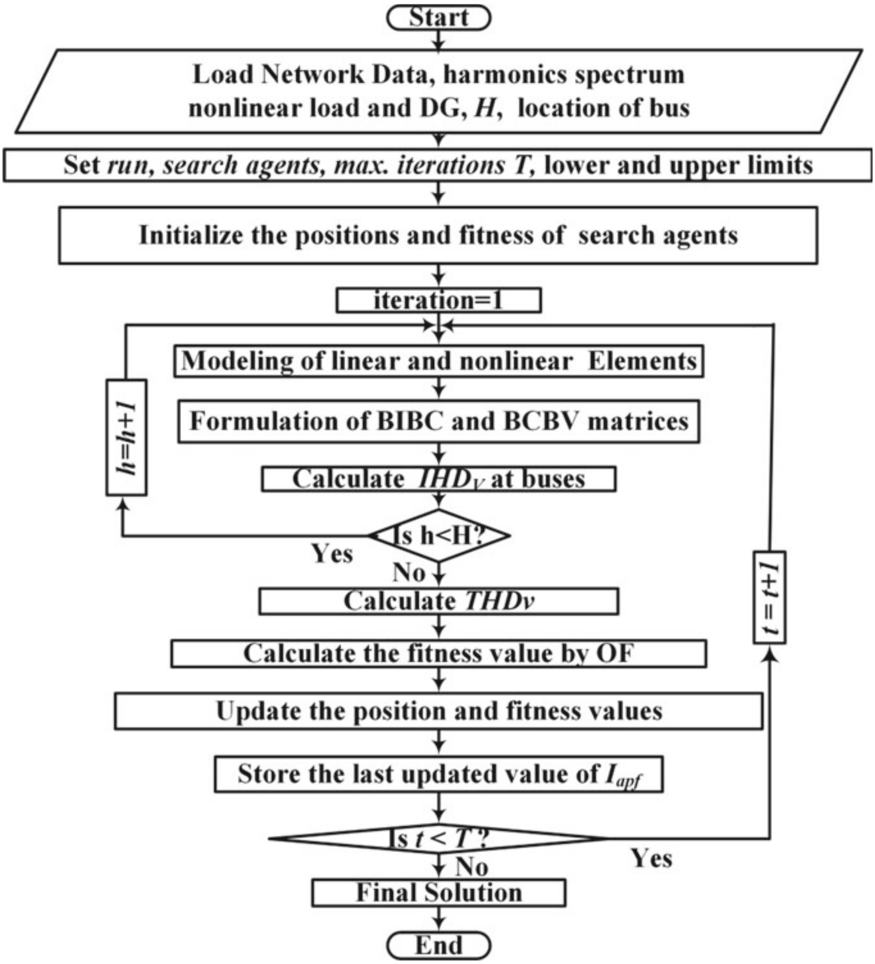

Fig. 2 Flowchart for OPAS of APF

5.2 *Result Analysis*

The NLs and NLDGs are connected at buses 27, 46, and 65. There are four different cases simulated; (i) Only NL (without APF), (ii) NL (With APF), (iii) NL plus NLDG (without APF), and (iv) NL plus NLDG (with APF).

Case 1 Only NL (without APF): In this case, only NLs are connected with RDS at buses 27, 46, and 65. The results obtained from THD_V without using APF are tabulated in Table 2. Bus 65 has a maximum THD_V (7.97%), compared to the other NL buses. Outs

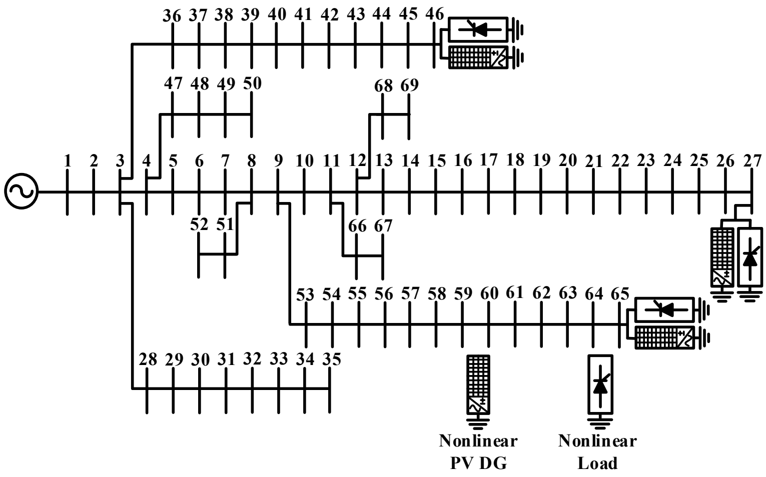

Fig. 3 IEEE-69 bus RDS with NLs and NLDGs

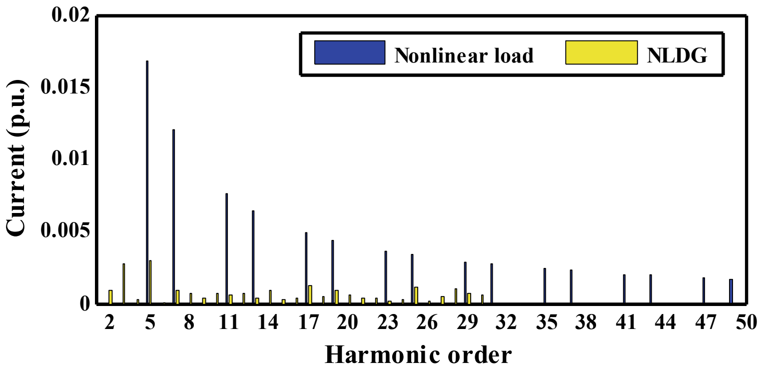

Fig. 4 Harmonics spectrum of NL and NLDG

Table 1 NLPCI matrix

State/APF bus	Number of APFs	27	46	65
1	One APF	+	*	*
2		*	+	*
3		*	*	+
4	Two APFs	+	+	*
5		+	*	+
6		*	+	+
7	Three APFs	+	+	+

"+" APF; "*" No APF

Table 2 THDv (%) at different buses (no APF)

Bus	THDv (%)	Bus	THDv (%)	Bus	THDv (%)	Bus	THDv (%)
2	0.01	19	**6.15**	36	0.04	53	2.26
3	0.02	20	**6.30**	37	0.37	54	2.48
4	0.03	21	**6.54**	38	0.62	55	2.79
5	0.15	22	**6.55**	39	0.70	56	3.09
6	0.94	23	**6.66**	40	0.70	57	4.24
7	1.77	24	**6.91**	41	2.49	58	4.80
8	1.97	25	**7.44**	42	3.25	59	**5.02**
9	2.07	26	**7.66**	43	3.35	60	**5.27**
10	2.65	27	**7.78**	44	3.38	61	**5.82**
11	2.79	28	0.02	45	3.67	62	**5.92**
12	3.29	29	0.02	46	3.67	63	**6.08**
13	4.02	30	0.02	47	0.03	64	**6.85**
14	4.75	31	0.02	48	0.03	65	**7.97**
15	**5.51**	32	0.02	49	0.03	66	2.79
16	**5.65**	33	0.02	50	0.03	67	2.79
17	**5.91**	34	0.02	51	1.97	68	3.29
18	**5.91**	35	0.02	52	1.97	69	3.29

of a total of twenty buses, THD_V exceeded 5% in all of them. It is an indication of a highly distorted system. These are beyond the limits as per the IEEE-519 standard. It shows the necessity of APF/APFs in this system.

Case 2 NL (With APF): To minimize the harmonics up to standard limits, according to Table 1, for states 1, 2, and 3, one APF; for states 4, 5, and 6, two APFs; and for state 7, three APFs are located as per NLPCI.

The size of the APFs is found using optimization methods at these placements. The TLBO, FPA, and BSA are employed in IEEE-69 bus RDS to test the computation performance. For considered algorithms, the common parameters—number of populations and total iterations are set to 40 and 100, respectively. Table 3 summarizes the best fitness value of an objective function for all the states. When the algorithms have not fulfilled the constraints, they exhibit a high value of the best fitness score as a result of the penalty applied. This effect of the penalty can also be observed in the early stages of the iterations (Fig. 7). After locating the APF/APFs, for states 1 to 3, only one APF, the algorithms are not converged as per Table 3. It shows that more

than one APF is needed to achieve the goal. For states 4 to 6, two APFS are located as per location matrix. Here, for state 4 and state 6, algorithms are not converged; i.e., two APFs at buses 27 and 46 for state 4; and at 46 and 65 for state 6 are no proper solutions to solve the problem.

For state 5 the algorithms are converged. For state 5, two APFs are at buses 27 and 65 the algorithms are converged. Among the optimization algorithms tested, the

Table 3 Comparison of the value of objective functions for both cases

State	Number of APFs and bus	Algorithm	I_{apf} (p.u.) (only NL)	I_{apf} (p.u.) (NL + NLDG)
1	One APF at 27	TLBO	29.6727	39.0036
		FPA	29.7775	39.3697
		BSA	29.6727	39.0036
2	One APF at 46	TLBO	54.4317	61.8787
		FPA	54.4317	61.8787
		BSA	54.4612	61.8787
3	One APF at 65	TLBO	27.3056	37.0769
		FPA	27.3271	37.1788
		BSA	27.3058	37.1088
4	Two APFs at 27 and 46	TLBO	29.5767	38.9426
		FPA	29.8321	39.4435
		BSA	37.2652	47.7294
5	**Two APFs at 27 and 65**	**TLBO**	**0.0184**	**0.0247**
		FPA	0.0245	0.0649
		BSA	0.0300	0.0500
6	Two APFs at 46 and 65	TLBO	27.1974	37.0102
		FPA	27.4594	38.3496
		BSA	27.8629	37.0813

best value was obtained using TLBO with a result of 0.0184 p.u., outperforming FPA (0.0245 p.u.), and BSA (0.0300 p.u.). It shows the limitation of BSA; it tends to suffer from premature convergence and easily gets trapped in local minima [10, 18]. Similarly, premature convergence and poor exploitation are shortcoming of FPA [19].

As per Table 3, for states 1 to 4 and 6, one APF and two APFs have not fulfilled the constraints; therefore, all three algorithms failed to converge. The algorithms are converged for state 5. As shown in Fig. 5, two APFs for state 5 fulfill the constraints, and all buses have THD_V less than 5%. It is found that the TLBO outperforms other algorithms in terms of performance.

Case 3 NL plus NLDG (without APF): The considered RDS is simulated with NLs and NLDGs. Due to the inclusion of NLDGs, the system is more distorted compared to only NL. Previously twenty buses have exceeded the acceptable limit for THD_V; but after incorporating NLDGs total of twenty-two buses have THD_V exceeded the standard

limit. It proves that the penetration of NLDG in RDS increases the harmonic distortion. As per Fig. 6, the maximum THD_V is observed at bus 65 (8.84%).

Case 4 NL plus NLDG (With APF): The scenario for state 5 is shown in Fig. 8. Here, two APFs are placed at buses 27 and 65. These two APFs have fulfilled the constraints.

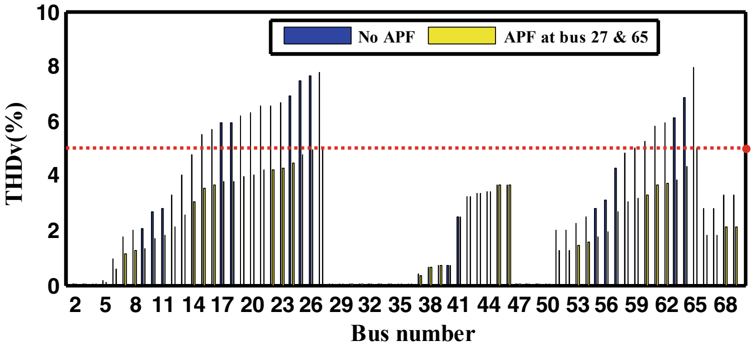

Fig. 5 THD$_V$ (%) at all buses without APF and placement of APF at buses 27 and 65 (only NL)

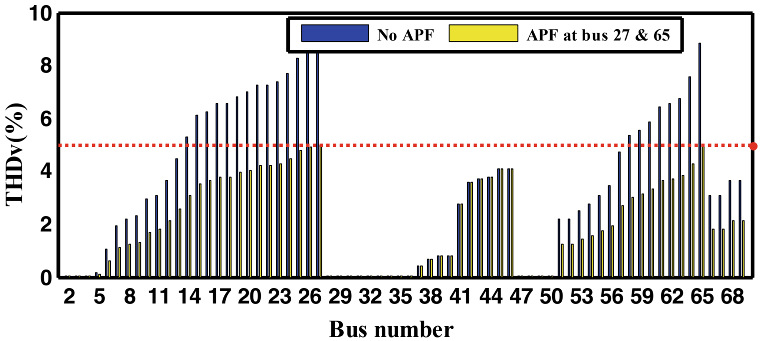

Fig. 6 THD$_V$ (%) at all buses without APF and placement of APF at buses 27 and 65 case 2 (NL plus NLDG)

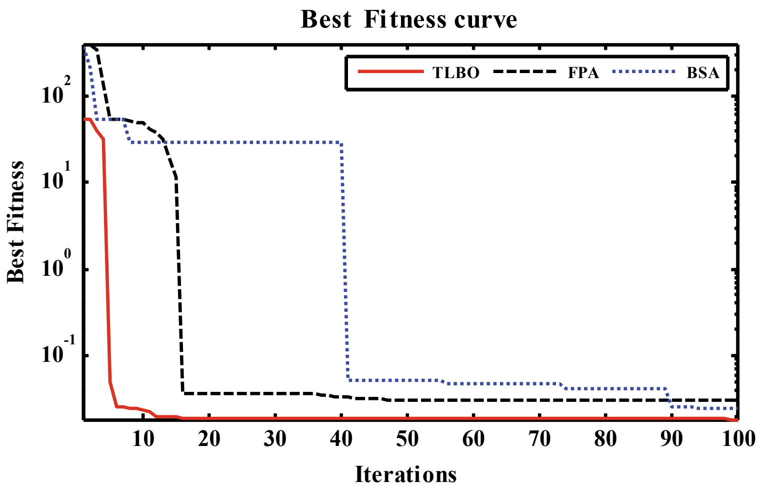

Fig. 7 Best fitness curve for State 5 (case 2)

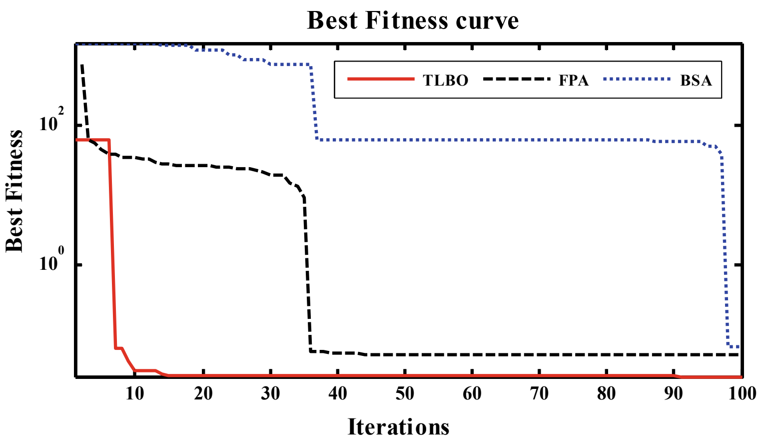

Fig. 8 Best fitness curve for state 5 (case 4)

All three algorithms have fulfilled the constraints for considered harmonic environment and converged. It is again proved that the TLBO has the lowest value compared to other considered algorithms. Out of the algorithms tested, TLBO produced the best value with a result of 0.0247 p.u., surpassing the results obtained with FPA (0.0649 p.u.) and BSA (0.0500 p.u.). It is also observed that the FPA and BSA are poor in the exploration phase compared to TLBO.

According to Table 3, it is clearly noticed that the inclusion of NLDG in RDS increases the harmonic distortion. The APFs required for this case have more ratings compared to case 2.

6 Conclusion

In this study, the OPAS of APF problem was effectively addressed using the TLBO algorithm, and its results were compared to those obtained from the FPA and BSA algorithms. The performance of the algorithms is demonstrated for NLs plus NLDGs in the IEEE-69 bus RDS. The TLBO algorithm implementation is straightforward and doesn't require adjusting any algorithm-specific parameters. The obtained numerical results have shown that TLBO has given the lowest APF current (0.0184 p.u. and 0.0247 p.u.). Also, it has a better convergence characteristic and the ability to converge near better optimal solution for the given problem. Moreover, it is observed that harmonic distortion is increased due to the addition of NLDGs in RDS. Therefore, the required APF current is also increased 1.34 times compared to NL only. The APF current has increased by a factor of 1.34 when compared to the scenario where only the NLs are present.

References

1. Hengsritawat V, Tayjasanant T, Nimpitiwan N (2012) Optimal sizing of photovoltaic distributed generators in a distribution system with consideration of solar radiation and harmonic distortion. Int J Electr Power Energy Syst 39:36–47
2. Kumar N, Kumar A (2017) Techno-economic analysis of non-linear DG penetration in radial distribution systems. Distr Gener Alternat Energy Journal 32:54–74
3. IEEE Recommended Practice and Requirements for Harmonic Control in Electric Power Systems. IEEE, New York, NY (2014)
4. Shivaie M, Salemnia A, Ameli MT (2014) A multi-objective approach to optimal placement and sizing of multiple active power filters using a music-inspired algorithm. Appl Soft Comput 22:189–204
5. Ziari I, Jalilian A (2010) A new approach for allocation and sizing of multiple active power-line conditioners. IEEE Trans Power Delivery 25:1026–1035
6. Lakum A, Mahajan V (2019) Optimal placement and sizing of multiple active power filters in radial distribution system using grey wolf optimizer in presence of nonlinear distributed generation. Electr Power Syst Res 173:281–290
7. Wolpert DH, Macready WG (1997) No free lunch theorems for optimization. IEEE Trans Evol Comput 1:67–82
8. Rao RV, Savsani VJ, Vakharia D (2011) Teaching–learning-based optimization: a novel method for constrained mechanical design optimization problems. Comput Aided Des 43:303–315
9. Yang X-S, Karamanoglu M, He X (2014) Flower pollination algorithm: a novel approach for multiobjective optimization. Eng Optim 46:1222–1237
10. Meng X-B, Gao XZ, Lu L, Liu Y, Zhang H (2016) A new bio-inspired optimisation algorithm: bird Swarm Algorithm. J Exp Theor Artif Intell 28:673–687
11. Teng J-H, Liao S-H, Leou R-C (2014) Three-phase harmonic analysis method for unbalanced distribution systems. Energies 7:365–384
12. Shivaie M, Salemnia A, Ameli MT (2013) Optimal multi-objective placement and sizing of passive and active power filters by a fuzzy-improved harmony search algorithm. Int Trans Electr Energy Syst 25:520–546
13. Sakar S, Balci ME, Aleem SHA, Zobaa AF (2017) Increasing PV hosting capacity in distorted distribution systems using passive harmonic filtering. Electr Power Syst Res 148:74–86
14. Sakar S, Balci ME, Aleem SHA, Zobaa AF (2018) Integration of large-scale PV plants in non-sinusoidal environments: considerations on hosting capacity and harmonic distortion limits. Renew Sustain Energy Rev 82:176–186
15. Savier J, Das D (2007) Impact of network reconfiguration on loss allocation of radial distribution systems. IEEE Trans Power Delivery 22:2473–2480
16. Fuchs E, Masoum MA (2011) Power quality in power systems and electrical machines. Academic press
17. Oliva AR, Balda JC (2003) A PV dispersed generator: a power quality analysis within the IEEE 519. IEEE Trans Power Delivery 18:525–530
18. Zhang D, Yang J, Yang P (2019) An improved chaos bird swarm optimization algorithm. J Phys Conf Ser 022016
19. Cui W, He Y (2018) Biological flower pollination algorithm with orthogonal learning strategy and catfish effect mechanism for global optimization problems. Math Prob Eng 2018